JOURNAL OF MATERIALS SCIENCE 20 (1985) 1859–1863

In situ conversion electron Mössbauer spectrometry (CEMS) studies on α- and γ-Fe_2O_3 gas sensors

MASANORI FUJINAMI, YUSUKE UJIHIRA
Department of Industrial Chemistry, Faculty of Engineering, The University of Tokyo, 7-3-1, Hongo, Bunkyo-ku, Tokyo 113, Japan

Clarification of the sensing mechanism of α-Fe_2O_3 and γ-Fe_2O_3 gas sensors was attempted. The information on the surface states of iron oxides at working temperature (400° C for α-Fe_2O_3 and 250° C for γ-Fe_2O_3) was obtained *in situ* by applying the *in situ* CEMS. The α-Fe_2O_3 gas sensor, prepared by the precipitation of $Fe(OH)_3$ from a solution of iron (III) sulphate and tin (IV) chloride, was composed of fine particles ($\simeq$ 15 nm) and was superior in sensitivity to other α-Fe_2O_3. The gas sensitivity was found to depend on the amounts of remaining sulphate ion, the microstructure and a small amount of iron (II) species generated through the reduction of α-Fe_2O_3. The sensing mechanism of γ-Fe_2O_3 gas sensor was confirmed to be due to the reduction of γ-Fe_2O_3 to the low resistive $Fe_{3-x}O_4$ by combustible gas and to depend on the crystal structure.

1. Introduction

It is known that oxide semiconductors exhibit gas sensitivities through variation of the electric resistivities by gas adsorption at high temperature [1–3]. α-Fe_2O_3 [4, 5] and γ-Fe_2O_3 [6] have attracted much attention as gas sensor materials because their surface resistivities decrease in an atmosphere of combustible gases such as CH_4, C_3H_8, i-C_4H_{10}, etc. However, little work has been carried out to elucidate the mechanism of the gas sensitive properties of these materials and a number of problems are left unsolved. In the present paper, we describe the results obtained by the application of conversion electron Mössbauer spectrometry (CEMS) to the *in situ* study of physical and chemical states of surface irons of α- and γ-Fe_2O_3 gas sensors. ^{57}Fe CEMS gives information on the surface states of the iron samples within several tens nm thick, because the penetration depth of 7.3 keV conversion electrons, re-emitted after recoilless resonant absorption of 14.4 keV γ-rays in the ^{57}Fe nucleus, is estimated to be about 100 nm in the iron oxides. The α-Fe_2O_3 and γ-Fe_2O_3 gas sensors work at 400 and 250° C, respectively, so that a new electron counter must be designed to obtain CEM spectra at high temperatures. Either an electron multiplier or a proportional counter was used to detect electrons in CEM measurement. Hitherto, Kowalski *et al.* [7] reported CEM measurements up to 927° C using electron multiplier, and Isozumi *et al.* [8] designed He–CO_2 gas proportional counter working up to 600° C by heating the whole counter. We also reported the fabrication of the gas flow type proportional counter for high temperature measurement by heating only the sample to reduce the possible thermal emission of electrons from the detector materials [9]. The temperature range we were interested in was up to 400° C in the present investigation, so we designed a new gas flow proportional counter having an advantage in the S/N ratio and stability for *in situ* measurement of a CEM spectrum. That is, the Fe_2O_3 sensor is mounted on the heater block over which helium containing a few percent of CH_4 or *i*-C_4H_{10} was passed. These organic gases work as a quenching gas as well as the reducible gas for sensing. A similar atmosphere to the working conditions of the gas sensor was achieved and *in situ* CEM studies were carried out. By comparison of the states of

0022–2461/85 $03.00 + .12

iron in the sensors at working temperature in the stream of He–CO_2 (10 vol %) with those in He–i–C_4H_{10} (1 vol %), their gas sensing mechanisms were estimated. The utility of the *in situ* CEMS was proposed and demonstrated in the present study.

2. Experimental techniques

2.1. Design and construction of the gas flow proportional counter

A schematic diagram of the counter designed is shown in Fig. 1. The counter material was aluminium and the window for the incident γ-ray was 20 μm thick aluminium foil. Only the sample holder, which was supported by two titanium tubes, was heated by a cartridge-type block heater (150 W) to reduce the emission of thermoelectrons from the counter wall. The outside of the counter was cooled by an electric fan so that the heat conduction from the heater to the counter materials was suppressed as much as possible. Teflon was used to insulate the anode from the cathode and was stable up to a working temperature of 400° C. The anode was the 50 μm diameter platinum wire, which was stretched out by a small spring in order to avoid loosening of the anode by the thermal expansion of the wire. The CA thermocouple was attached to a sample and the temperature was regulated to within ± 2° C using the thermo-controller.

Generally, the counting gas must have both properties to ensure stable gas ionization and not to change the surface condition of the samples at working temperature. He–CO_2 (10 vol %) was used as a counting gas because it was reported to be inert to the iron oxides up to 600° C and to show good counting characteristics [8]. The voltage applied to the anode in the stream of He–CO_2 was 1500 and 1300 V at RT and 400° C, respectively. He–i-C_4H_{10} (1 vol %), to which the α-Fe_2O_3 and the γ-Fe_2O_3 gas sensors are sensitive, also worked as a counting gas. Therefore, He–CO_2 was passed into the counter to obtain the blank of the sensor response and He–i-C_4H_{10} for *in situ* CEM studies of the sensor surface at high temperature. The applied voltage in He–i-C_4H_{10} was 1000 and 800 V at RT and 400° C, respectively. The temperature elevation of the sample required application of a lower voltage in this temperature range, as the mean free path of electrons became longer. A ^{57}Co/Rh γ-ray source (10 mCi) was fixed to a conventional Mössbauer spectrometer. The fabricated gas flow proportional counter gave a perfect performance in the temperature range up to 400° C. The Mössbauer spectra obtained were computer-fitted assuming the Lorentzian shape to the peaks. Doppler velocity was calibrated with reference to α-Fe at room temperature.

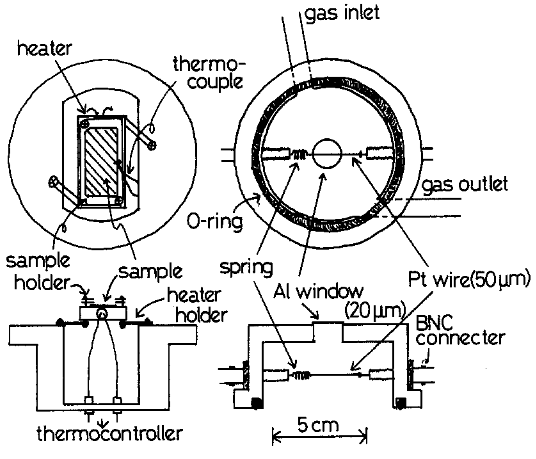

Figure 1 Schematic illustration of a new proportional counter for high temperature CEM measurement.

2.2. Sample preparations

2.2.1. α-Fe_2O_3 gas sensor

Three different α-Fe_2O_3 specimens (samples A, B and C) were prepared from the aqueous solutions of $Fe(NO_3)_3 \cdot 9H_2O$, $Fe_2(SO_4)_3 \cdot nH_2O$ and a mixture of $Fe_2(SO_4)_3 \cdot nH_2O$ and $SnCl_4 \cdot nH_2O$ (20 mol %), respectively. Ammonium solution was added dropwise to the solution of the respective iron salt at 50° C until the pH of the solution became 7.2. The precipitate was filtered, washed, dried, ground in an agate mortar and calcined in air at 400° C for 1 h. The resulting powders were pressed into pellets (20 mm diameter, 1 mm thick) at a pressure of 10^3 kg cm^{-2} and sintered in air at 600° C for 1 h.

2.2.2. γ-Fe_2O_3 gas sensor

Powders of Fe_3O_4 were pressed into pellets (20 mm diameter, 1 mm thick) at a pressure of 10^3 kg cm^{-2}, sintered in vacuum at 700° C for 1 h and then oxidized to γ-Fe_2O_3 by heating in air at 250° C for 24 h.

3. Results and discussion

3.1. α-Fe_2O_3 gas sensor

Ordinary α-Fe_2O_3 does not show a sensitivity to reducible gases, but α-Fe_2O_3 prepared from iron sulphate solution has a gas sensitive property,

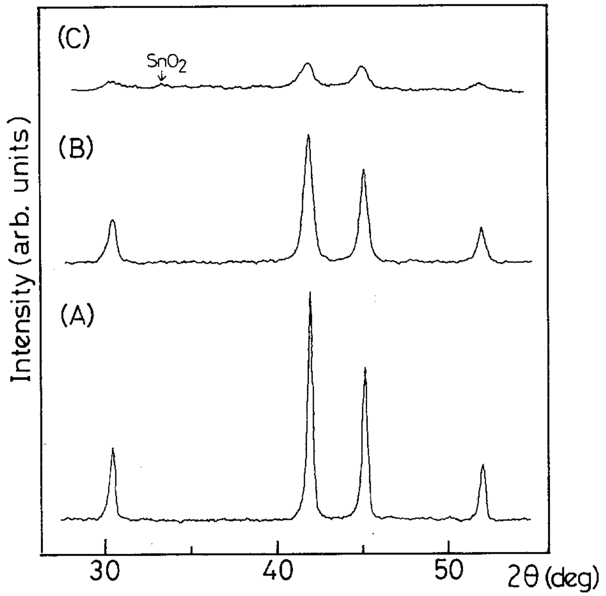

Figure 2 X-ray diffraction patterns of different α-Fe_2O_3 specimens prepared from (A) $Fe(NO_3)_3 \cdot 9H_2O$, (B) $Fe_2(SO_4)_3 \cdot nH_2O$ and (C) $Fe_2(SO_4)_3 \cdot nH_2O + SnCl_4 \cdot nH_2O$. (Target: Fe.)

which can be enhanced by the inclusion of Sn(IV), Zr(IV) or Ti(IV) in it. Properties of three different α-Fe_2O_3 specimens (samples A, B and C) prepared from different iron solutions were investigated and compared. The resistivity of sample B, prepared from $Fe_2(SO_4)_3 \cdot nH_2O$, decreased by about one order of magnitude in the atmosphere of 1 vol% i-C_4H_{10} at 400° C, and that of sample C, prepared from the mixture of $Fe_2(SO_4)_3 \cdot nH_2O$ and $SnCl_4 \cdot nH_2O$ (20 mol%), changed more remarkably, while sample A, prepared from $Fe(NO_3)_3 \cdot 9H_2O$, showed little variation in resistivity. Figs. 2 and 3 show X-ray diffraction (XRD) patterns and CEM spectra of three different α-Fe_2O_3 specimens at RT. The diffraction peaks of the gas sensitive sample B were broader than those of non-sensitive sample A. The internal magnetic fields (H_f) of samples A and B were calculated as 51.5 and 50.3 T, respectively. Both the broadness of the XRD peaks and the decrease of the internal magnetic fields in CEM spectra indicated that the particle size was finer. The sulphate ion was considered to play an essential role in the formation of fine particles of α-Fe_2O_3 and the generation of a gas sensitivity. However, the chemical differences between samples A and B could not be observed and the chemical state of sulphate ion could not be clarified in the present investigation. On the other hand, the broadness was more remarkable for sample C, which has the best gas sensitivity, and the peaks due to SnO_2 appeared in the XRD pattern. The CEM spectrum of sample C consisted of magnetically split peaks ($IS = 0.35\ \mathrm{mm\,sec^{-1}}$, $QS = 0.35\ \mathrm{mm\,sec^{-1}}$, $H_f = 49.5$ T) and doublet peaks ($IS = 0.35\ \mathrm{mm\,sec^{-1}}$, $QS = 0.68\ \mathrm{mm\,sec^{-1}}$), which showed the presence of superparamagnetic α-Fe_2O_3 particles. The relaxation time, τ_0, between spin flips is proportional to $\exp(2KV/kT)$, where K is the anisotropy constant and V is the particle volume. For $\tau_{obs} \gg \tau_0$, the particles indicate the superparamagnetism. The average particle diameter of α-Fe_2O_3, at which superparamagnetic behaviour was shown at RT, was estimated to be about 13.5 nm by Kündig *et al.* [10]. The percentage of superparamagnetic fraction, $A_{super}/(A_{ferro} + A_{super})$, in sample C was 35%

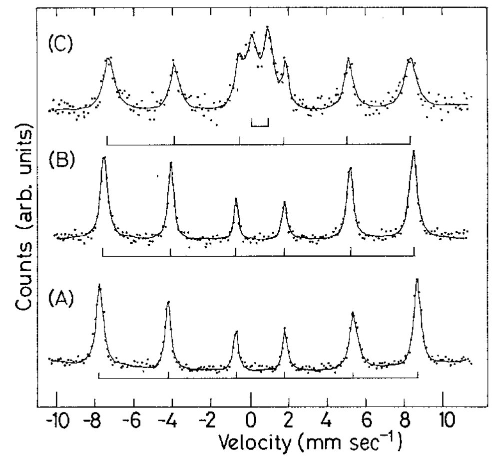

Figure 3 CEM spectra of different α-Fe_2O_3 specimens at RT prepared from (A) $Fe(NO_3)_3 \cdot 9H_2O$, (B) $Fe_2(SO_4)_3 \cdot nH_2O$ and (C) $Fe_2(SO_4)_3 \cdot nH_2O + SnCl_4 \cdot nH_2O$.

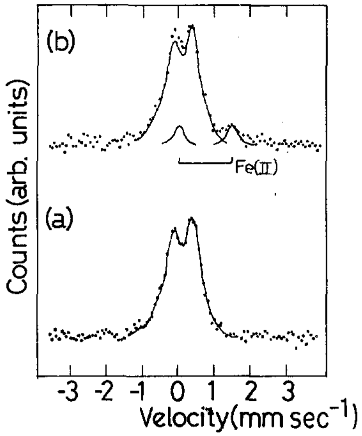

Figure 4 CEM spectra of α-Fe_2O_3 gas sensor prepared from $Fe_2(SO_4)_3 \cdot nH_2O + SnCl_4 \cdot nH_2O$ observed at 400° C in (a) He–CO_2(10 vol%) and in (b) He–i-C_4H_{10} (1 vol%).

and the average particle diameter was estimated to be not more than about 15 nm. The addition of Sn(IV) restrained the growth of particles of α-Fe_2O_3 and controlled the microstructure. The addition of Ti(IV) or Zr(IV) in the α-Fe_2O_3 brought about similar results, but Sn(II) did not give such an effect to it.

α-Fe_2O_3 is an n-type semiconductor, in which the conduction electrons are generated by the formation of an oxygen ion vacancy in accordance with the following equilibrium equation:

$$O_O = \tfrac{1}{2} O_2(g) + V_O^{\cdot\cdot} + 2e',$$

where the Kroeger–Vink notation is used. Assuming that a quadrivalent metal such as Sn(IV) is added to Fe_2O_3 in solid solution, the following reaction is given:

$$SnO_2 = 2\,Sn_{Fe}^{\cdot} + Fe_2O_3 + \tfrac{1}{2} O_2(g) + V_{Fe}''$$

As the diffusion coefficient is proportional to the vacancy concentration, the sintering rate increases and is generally proportional to the inverse of the particle size [11]. As a result, the grain growth of the α-Fe_2O_3 particle is considered to be restrained by the addition of Sn(IV).

The CEM spectra of three different α-Fe_2O_3 specimens were observed at 400° C in a stream of He–CO_2 (10 vol%) and He–i-C_4H_{10} (1 vol%). No differences appeared in the CEM spectra on variation of the flow gas to samples A and B. Fig. 4 shows *in situ* CEM spectra of sample C at 400° C in a stream of He–CO_2 (a) and He–i-C_4H_{10} (b). The Néel temperature of α-Fe_2O_3 is 688° C [12]. However, only the doublet peaks (IS = 0.18 mm sec^{-1}, QS = 0.50 mm sec^{-1}), showing superparamagnetism due to fine particles of α-Fe_2O_3, were observed, as shown in Fig. 4a. The doublet peaks (IS = 0.85 mm sec^{-1}, QS = 1.53 mm sec^{-1}) due to Fe(II) species were slightly observed in the CEM spectrum by flowing He–i-C_4H_{10} at 400° C, as shown in Fig. 4b. This result indicated that a small amount of Fe(II) compound was produced by the reduction of fine α-Fe_2O_3 particles at the sensor surface and caused the resistivity change of sensor materials. However, it entails further studies to elucidate the correlation of the sulphate ion and the microstructure with the production of Fe(II) species and the gas sensing mechanism of α-Fe_2O_3.

3.2. γ-Fe_2O_3 gas sensor.

The γ-Fe_2O_3 sensor had a porous structure and the value of the resistance decreased from $2.5 \times 10^7\,\Omega$ to $1.2 \times 10^6\,\Omega$ in the atmosphere of 1 vol% i-C_4H_{10} at 250° C within 5 min. Fig. 5 shows CEM spectra of γ-Fe_2O_3 sensors kept in He–CO_2 (10 vol%) at RT (a), in He–CO_2 (10 vol%) at 250° C (b), and in He–i-C_4H_{10} (1 vol%) at 250° C (c). The CEM spectrum observed at RT was composed of only one magnetically split sextet with IS = 0.45 mm sec^{-1} and $H_f = 50.2$ T showing the sole presence of γ-Fe_2O_3 phase at the surface. The CEM spectrum measured at 250° C (Fig. 5b) also consisted of one sextet with IS = 0.25 mm sec^{-1} and $H_f = 45.4$ T. It indicated that γ-Fe_2O_3 was kept unchanged chemically by the thermal treatment. When the CEM spectrum of the γ-Fe_2O_3 sensor was measured under the working conditions of flowing He–i-C_4H_{10} at 250° C, two sextets were observed in addition to the sextet due to γ-Fe_2O_3, as shown in Fig. 5c. New sextets were assigned to $Fe_{3-x}O_4$ from their Mössbauer parameters (A site, IS = 0.45 mm sec^{-1}, H_f = 44.5 T; B site, IS = 0.60 mm sec^{-1}, H_f = 41.6 T). These results revealed that the γ-Fe_2O_3 present at the surface of the sensor was reduced to $Fe_{3-x}O_4$, which had a low resistivity, in the reducible atmosphere. They also confirmed the gas sensing mechanism proposed by Matsuoka *et al.* [6]. Both $Fe_{3-x}O_4$ and γ-Fe_2O_3 have an inverse spinel structure and the reversible transformation between them occurred easily at relatively low temperatures. According to our results, the change in resistivity of the γ-Fe_2O_3 sensor was caused by the change of chemcial composition (reduction of

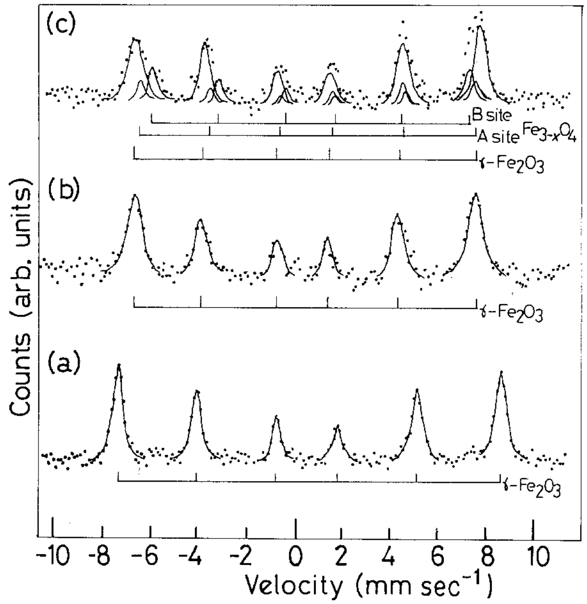

Figure 5 CEM spectra of γ-Fe_2O_3 gas sensor, (a) at RT in He–CO_2 (10 vol%), (b) at 250° C in He–CO_2 (10 vol%), (c) at 250° C in He-*i*-C_4H_{10} (1 vol%).

γ-Fe_2O_3 to $Fe_{3-x}O_4$) at the particle surfaces and the facility of the reduction depended on the crystal structure. On the other hand, the gas sensitivity of ZnO and SnO_2 sensors was considered to be caused by the change of the potential barrier due to the adsorption and desorption of oxygen and also dependent on their microstructure.

4. Conclusions

The *in situ* CEMS studies confirmed the sensing mechanism of α- and γ-Fe_2O_3 gas sensors as follows.

1. The α-Fe_2O_3 gas sensor, which is prepared by the precipitation of iron hydroxide from a solution of Fe(III) sulphate and Sn(IV) chloride, is composed of fine particles ($\simeq$ 15 nm diameter) of α-Fe_2O_3. The sulphate ion and the microstructure of fine particles play important parts in the sensing mechanism and the decrease of resistivity was caused by the production of a small amount of Fe(II) species, although the conduction mechanism cannot yet be clearly solved.

2. The redox reaction between γ-Fe_2O_3 and $Fe_{3-x}O_4$ at the surfaces of γ-Fe_2O_3 particles is responsible for the change of resitivity of the γ-Fe_2O_3 sensor and the gas sensitivity depended on the crystal structure.

The information on the surface states of gas sensors was obtained *in situ* by means of CEMS applied at high temperature. The authors are planning the application of this technique to the charaterization of a tin oxide gas sensor and iron catalysts for the Fischer–Tropsch reaction by flowing a mixture of He, CO and H_2 as counting gas and reactant.

References

1. C. WAGNER, *J. Chem. Phys.* **18** (1950) 69.
2. K. HAUFFE and H. ENGELL, *Z. Electrochem.* **56** (1952) 366.
3. T. SEIYAMA, A. KATO, K. FUJIISHI and M. NAGATANI, *Anal. Chem.* **34** (1962) 1502.
4. Y. NAKATANI and M. MATSUOKA, *Jap. J. Appl. Phys.* **21** (1982) L758.
5. Y. NAKATANI, M. SAKAI and M. MATSUOKA, *ibid.* **22** (1983) 912.
6. M. MATSUOKA, Y. NAKATANI and H. OHIDO, *Nat. Tech. Rep.* **24** (1978) 461.
7. J. KOWALSKI, J. STANEK, T. TYLISZCZAK and J. A. SAWICKI, *Nucl. Instrum. Methods* **216** (1983) 299.
8. Y. ISOZUMI, M. KURAKADO and R. KATANO, *Rev. Sci. Instrum.* **52** (1981) 413.
9. M. INABA, H. NAKAGAWA and Y. UJIHIRA, *Nucl. Instrum. Methods* **180** (1981) 131.
10. W. KÜNDIG, H. BÖMMEL, G. CONSTABARIS and R. H. LINDQUIST, *Phys. Rev.* **142** (1966) 327.
11. W. D. KINGERY, H. K. BOWEN and U. R. UHLMANN, "Introduction to Ceramics", 2nd Edn. (John Wiley, New York, 1976) p. 448.
12. C. M. ISERENTANT, G. G. ROBBRECHT and R. J. DOCLO, *Phys. Lett.* **11** (1964) 14.

Received 17 June
and accepted 6 July 1984